Vol. 33 • No. 51 • December 15 • 2023

www.afm-journal.de

ADVANCED FUNCTIONAL MATERIALS

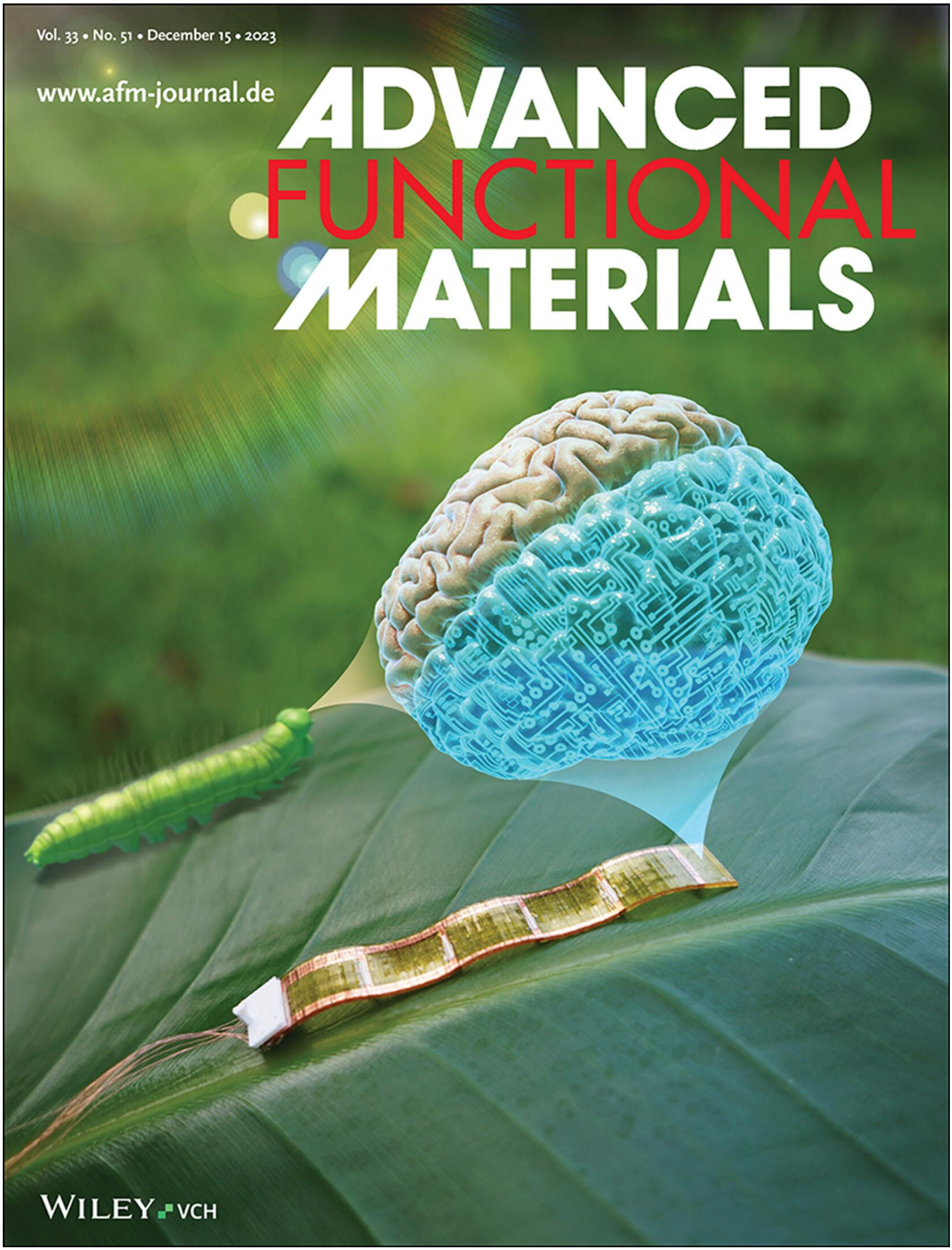

WILEY VCH

Bitumen-Like Polymers Prepared via Inverse Vulcanization with Shear Stiffening and Self-Healing Abilities for Multifunctional Applications

Ke-Xin Hou, Pei-Chen Zhao, Lei Duan, Minjie Fan, Pengfei Zheng, Cheng-Hui Li

2306886 | First Published: 08 September 2023

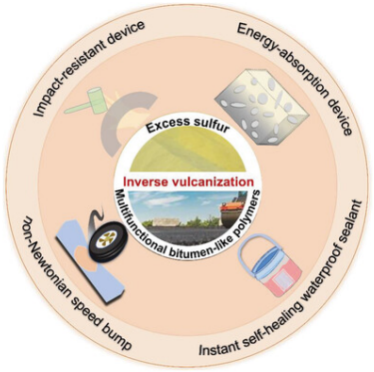

A series of bitumen-like polymers are obtained through inverse vulcanization. Based on extra shear stiffening performance and self-healing ability, they show great potential in impact-resistant devices, energy-absorption devices, self-healing waterproof sealants, and non-Newtonian speed bumps which can solve simultaneously the challenging problem of bitumen's unsustainability as well as sulfur's utilization.

Abstract | **Full text** | **PDF** | **References** | **Request permissions**

Tough Yet Reversible Hydrogel Adhesives with Cooperative Energy Dissipation for Multifunctional Wearable Sensors

Gang Lu, Qi Zhu, Rui Ma, Wei He, Jun Wu

2306914 | First Published: 13 September 2023

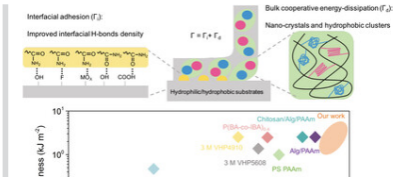

A strategy of cooperative energy dissipation is reported to prepare phase-segregated hydrogel adhesives that are prepared via varying times of solvent exchange followed by dry-annealing and reswelling. Abundant nano-aggregates in the bulk comprising hydrophobic clusters and hydrogen-bonded nanocrystals allow for

ADVANCED FUNCTIONAL MATERIALS
www.afm-journal.de

Bitumen-Like Polymers Prepared via Inverse Vulcanization with Shear Stiffening and Self-Healing Abilities for Multifunctional Applications

Ke-Xin Hou, Pei-Chen Zhao, Lei Duan, Minjie Fan, Pengfei Zheng, and Cheng-Hui Li**

Bitumen, which is widely used in various applications, is facing the challenge of being unsustainable. Many strategies are proposed to recycle or replace bitumen. However, most of them can not address the unsustainability of bitumen from the roots. On the other hand, sulfur exists widely on the earth as a kind of industrial waste despite its extensive applications. Herein, a series of bitumen-like polymers from elemental sulfur is obtained through an inverse vulcanization reaction. The sulfur-containing polymers exhibit self-healing, non-toxic, and adjustable properties depending on the working environment. Based on these features, the applications of sulfur-containing polymers in self-healing waterproof sealants, impact-resistance or shock-absorption devices, and non-Newtonian speed bumps are demonstrated. With the method of synthesizing multifunctional bitumen-like polymers from sulfur wastes, a feasible way is provided to solve simultaneously the challenging problem of bitumen's unsustainability as well as sulfur's utilization, with the advantages including easy massed-fabrication, non-toxicity, extremely low cost (≈2 cents per gram) and environment friendliness.

1. Introduction

Bitumen is a viscoelastic organic liquid material refined from petroleum and has been widely used in coatings, plastics, rubber, road pavements, and other industries.[1–7] Particularly, with the fast development of road construction, the proportion of asphalt pavement in road engineering is increasing due to its advantages such as convenient construction and comfortable driving (**Figure 1**A).[8,9] However, bitumen generally derives from petroleum, which is an unsustainable resource and is progressively depleting. The production of bitumen is a high-temperature and resource-intensive process during which the toxic bitumen fumes and vapors may be released and thus harmful to the workers.[10–14] Moreover, a large amount of (carbon dioxide) CO_2 is emitted (0.048 $kgCO_2eq/kg$) during the production and processing of bitumen.[15,16] Most of the paved roads in the world are made of bitumen which causes huge emission of CO_2 and is unfavorable for protecting the environment.[15] Many strategies, such as recycling the waste asphalt by adding reactive chain extension rejuvenators, or utilizing biomaterials to replace bitumen in asphalts mixtures, can effectively reduce the amount of bitumen consumption.[17–19] However, such methods can not address the unsustainability of bitumen from the roots. It is essential to develop simple, low-cost, non-toxic methods to synthesize bitumen or bitumen-like materials with abundant or renewable resources.

On the other hand, sulfur is widely distributed in nature, with a content of 0.048% (by mass) in the crust. More than 60 million tons of sulfur are produced annually, most of which are by-products from the hydrodesulfurization process in reducing sulfur dioxide emissions from the combustion of fossil fuels in the oil refinement and gas purification processes.[20,21] Owing to its unique properties, sulfur is useful in many fields, such as being an excellent fungicide to treat various garden pests and diseases,[22] reacting with other elements to form valuable compounds,[23] acting as the curing ingredient for vulcanization of rubber,[24] functioning as the cathode in lithium–sulfur batteries or sodium–sulfur batteries,[25] etc. When prepared as quantum dots, sulfur can also be utilized in bioimaging, sensing, catalytic activity, and fabrication of light-emitting devices.[26–30] In spite of its widespread applications, there is still an excess of 7 million tons of element sulfur each year and the majority of which is stored in the surface sediments in the form of powder (Figure 1B).[31] It is highly desirable to realize the efficient utilization of these sulfur wastes by finding a pathway to consume large amounts of sulfur.

K.-X. Hou, P.-C. Zhao, C.-H. Li
State Key Laboratory of Coordination Chemistry
School of Chemistry and Chemical Engineering
Collaborative Innovation Center of Advanced Microstructures
Nanjing University
Nanjing 210023, P. R. China
E-mail: chli@nju.edu.cn

L. Duan
School of Chemical Engineering and Materials
Changzhou Institute of Technology
Changzhou 213032, P. R. China

M. Fan, P. Zheng
Department of Orthopedic Surgery
Children's Hospital of Nanjing Medical University
Nanjing 210000, P. R. China
E-mail: zhengpengfei@njmu.edu.cn

The ORCID identification number(s) for the author(s) of this article can be found under https://doi.org/10.1002/adfm.202306886

DOI: 10.1002/adfm.202306886

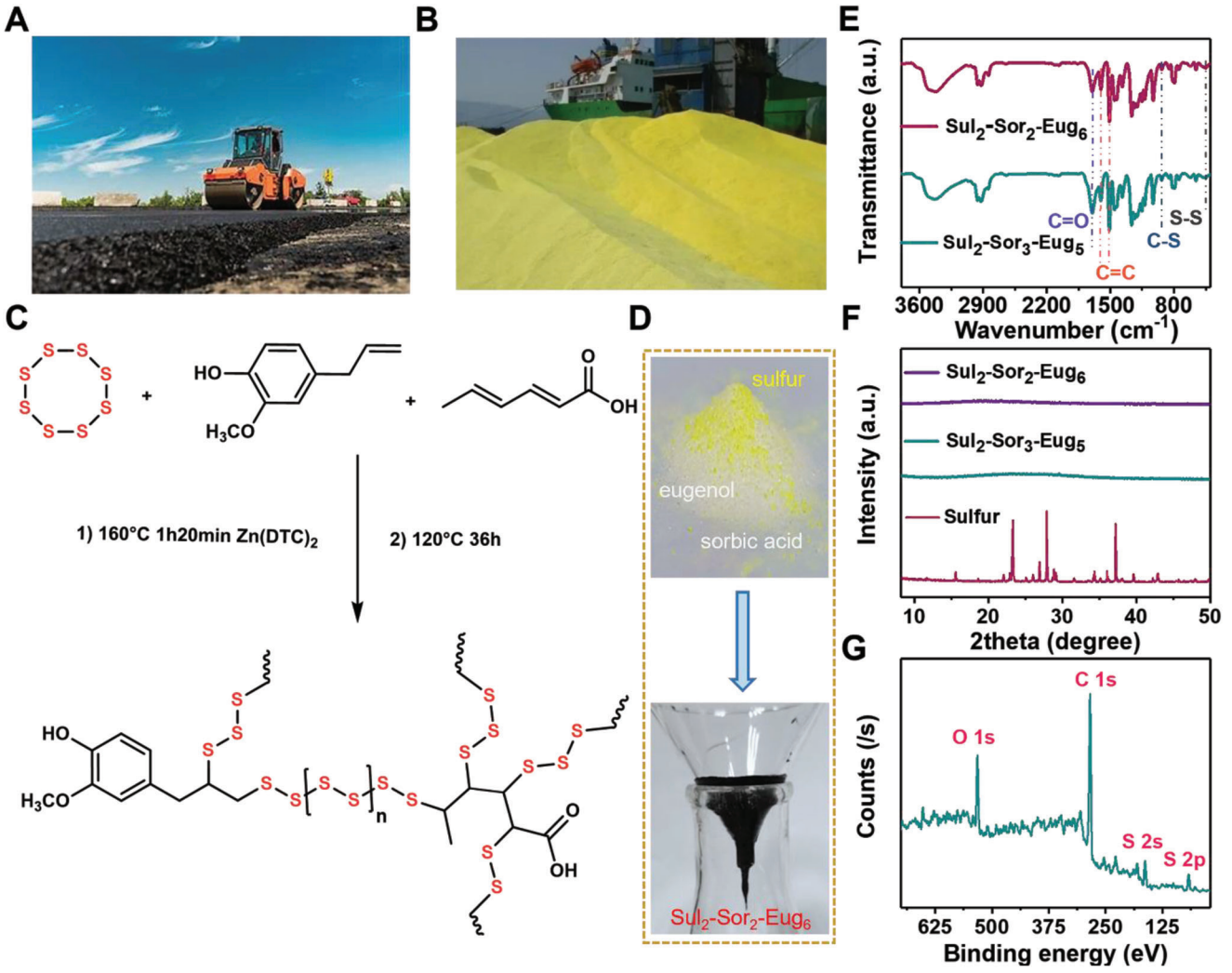

Figure 1. Synthesis and characterization of sulfur-containing polymer Sul-Sor-Eug. A) Scene of asphalt paving. B) Optical picture of a large amount of sulfur waste accumulation. C) Schematic structure of Sul-Sor-Eug. D) Optical photos of raw materials before reaction and products after reaction. E) FT-IR spectra of Sul-Sor-Eug (C═C in right, C═O in purple, C—S in blue, and S—S in gray). F) PXRD patterns Sul-Sor-Eug. G) Full spectrum of Sul_2-Sor_2-Eug_6.

In the 1970s, sulfur was used as a partial replacement for bitumen (called sulfur-extended asphalt, SEA) to reduce the high costs of bitumen because of its advantage in reducing mixing and compaction temperature.[32] However, the sulfur in SEA is easy to depolymerize into S_8 through the back-biting mechanism. To improve the stability of sulfur elements within bitumen, Fini et al. proposed a method utilizing the double bond in waste cooking oil which could react with sulfur elements in SEA by free radical addition reaction.[33] They also reported that phenolic compounds derived from plant-based sources can hinder the formation of sulfur dendritic structures and inhibit the process of sulfur crystallization, mainly due to that the phenoxyl radicals with electron delocalization and hydrogen donation property can neutralize the polysulfide radicals.[34] Based on these results, we aspire to combine the element sulfur and phenolic compounds to directly obtain bitumen substitutes. According to statistics, more than 90% of pavements in the world use asphalt binder.[35] Deriving bitumen substitutes from sulfur can not only achieve a large conversion of waste sulfur but also solve the unsustainable sources of bitumen, which is beneficial to sustainable development and resource conservation.

Herein, we use sorbic acid, eugenol, and sulfur to prepare a series of polymers with a sulfur content of 20% (wt.%) through inverse vulcanization. The obtained sulfur-containing polymers have similar properties to 70# bitumen but show lower toxicity, better resistance to permanent deformation, higher temperature resistance to rutting, higher temperature sensitivity, and better stability in water environment. Moreover, these polymers show shear stiffening and self-healing performance due to the presence of both flexible chains and rigid aromatic domains as well as dynamic hydrogen bonds. The properties of these bitumen-like polymers can further be tuned by the introduction of coordination bonds. We then demonstrated their applications in self-healing waterproofing sealants, impact-resistant materials, and non-Newtonian speed bumps. Along with the intriguing properties and useful applications, the synthesis of the bitumen-like polymers is extremely low cost (≈2 cents per gram) and can be easily scaled up. These features are desirable for converting

excessive sulfur into multifunctional products and overcoming the unsustainable problem of bitumen.

2. Results and Discussion

2.1. Material Synthesis and General Characterization

The bitumen-like polymers were prepared via inverse vulcanization reaction. As we all know, the element sulfur exists in the form of an eight-membered ring at room temperature and melts into a clear yellow liquid phase at 121–124 °C.[36] Upon further heating to the floor temperature (159 °C), the element sulfur will undergo ring-opening polymerization, forming a linear polysulfide with sulfur radicals at both ends.[31,36] This form is unstable and will quickly depolymerize into S_8 through a backbiting mechanism.[36] Pyun et al. have innovatively proposed an "inverse vulcanization" method for preparing polymers with high sulfur content and stable performance by polymerization of sulfur and diene-based comonomers which has attracted many researchers.[31,37] Divinyl and sulfur were cross-linked through free radical reaction which effectively prevents the depolymerization of polysulfide chains.[38] Here, eugenol and sorbic acid were chosen to inhibit the depolymerization of linear polysulfide chains and control the crosslink density of the polymer (Figure 1C). Eugenol is non-toxic, abundant, and easily accessible in nature which can not only provide better compatibility with liquid sulfur due to the aryl moieties but also inhibit the process of sulfur crystallization owing to the presence of phenoxyl radicals.[34,39–41] Sorbic acid is also non-toxic and widely used in food and cosmetics as a preservative, and the diene group of sorbic acid can effectively inhibit the process of sulfur depolymerization by crosslinking the sulfur.[42–45] Besides, the rigid benzene ring unit in eugenol can be used to improve the mechanical strength and the carboxyl groups in sorbic acid can be used to provide hydrogen bonding to improve the viscosity. Zn $(DTC)_2$ (Zn diethyldithiocarbamate) has been reported as the effective inverse vulcanization accelerator and therefore was chosen as the catalyst.[46] Based on the monomer content, we named the polymerized product Sul_x-Sor_y-Eug_z (The total amount of polymer is set to 10, x, y, z represents the mass content of each component, respectively). As shown in Figure 1C, the reaction process includes two steps: reacting at 160 °C and then curing at 120 °C. The two steps, corresponding to the initial ring-opening polymerization stage at the floor temperature (159 °C) and the curing stage at the melting point (120 °C) of sulfur, are designed to ensure that the residual sulfur in the system can be completely consumed. The sample is rigid solid when $z \geq 7$, and turns into viscous liquid when $y \geq 4$. Upon comprehensive consideration, Sul_2-Sor_2-Eug_6 and Sul_2-Sor_3-Eug_5 were chosen as the optimized recipes in our study. The optical pictures of Sul_2-Sor_2-Eug_6 before and after the reaction are shown in Figure 1D.

The Fourier transform IR (FT-IR) spectrum of the reaction product is shown in Figure 1E. The stretching vibration bands at 939 and 451 cm^{-1} are assigned to the C—S and S—S stretching vibration absorption peaks, respectively.[47] The spectrum also shows peaks at 1601 and 1511 cm^{-1}, corresponding to the skeleton stretching vibration of the benzene ring in eugenol. In addition, there is a characteristic band at 1692 cm^{-1} which is ascribed to the C═O stretching vibrations in sorbic acid. These results prove that the C═C bonds have been consumed completely and new C—S bonds have been formed. Elemental analysis was conducted to assess the loss of H_2S generated during the reaction. The results of Sul_2-Sor_2-Eug_6 are shown in Table S1 (Supporting Information). The theoretical hydrocarbon ratio of Sul_2-Sor_2-Eug_6 is calculated to be 9.75: 1, while the actual hydrocarbon ratio is 9.95: 1. Therefore, there was 2.023% H_2S loss in the inverse vulcanization reaction. Furthermore, the ^1H NMR spectrum of Sul_2-Sor_3-Eug_5 in Figure S1 (Supporting Information) also manifests the completion of the polymerization reaction. As shown in Figure S2 (Supporting Information), pure sulfur underwent a solid–solid orthorhombic–monoclinic transformation at ≈106 °C and melted after further heating at 118 °C. Both peaks disappeared in the DSC curve of the polymer, indicating that the crystalline sulfur had been completely converted into bitumen-like polymers (Figure S3, Supporting Information). The glass transition temperature of the polymer varied from −3.16 to 4.36 °C depending on the content of each component, which may be related to the crosslinking density and the amount of aromatic ring (Figure S3, Table S2, Supporting Information). Assuming that each C═C bond formed two C—S bonds, the calculated polysulfide ranks of Sul_6-Sor_2-Eug_2, Sul_4-Sor_2-Eug_4, Sul_2-Sor_2-Eug_6, Sul_2-Sor_3-Eug_5, and Sul_2-Sor_4-Eug_4 are 3.24, 2.41, 1.43, 1.38 and 1.33, respectively.[23] PXRD (Powder X-Ray Diffraction) and TGA (thermogravimetric analysis) further proved that no unreacted crystalline sulfur remained in the polymer networks, as shown in Figure 1F and Figure S4 (Supporting Information). Therefore, it can be concluded that the sulfur-containing polymers were successfully synthesized.

XPS (X-ray photoelectron spectroscopy) was performed to collect further information about the bond connectivity within the polymer matrix. There are characteristic peaks of S 2p, C 1s, O 1s, and S 1s in the XPS survey spectrum as shown in Figure 1G. High-resolution XPS analysis for each element was also conducted, where the C 1s was deconvoluted to C—O, C—C/C═C, C—S, and C—O at 286.30, 284.72, 285.55, and 287.19 eV (Figure S5A, Supporting Information), respectively.[48] The S 2p peak was deconvolved into two doublets as shown in Figure S5B (Supporting Information), with the binding energy of S—S and C—S bonds found at 165.21/163.88 eV and 164.7/163.03 eV, respectively.[48] In addition, the O1s spectrum only shows a single peak (Figure S5C, Supporting Information), indicating that no sulfur oxides are formed during the polymerization process.[23] Besides, we have conducted dissolution experiments in different solvents including *n*-Hexane, toluene, (dichloromethane) DCM, (tetrahydrofuran) THF, acetone, (ethyl alcohol) EtOH, (*N, N*-Dimethylformamide) DMF, (dimethyl sulfoxide) DMSO, and H_2O. The mass of Sul_2-Sor_3-Eug_5 is set to be 0.3 g and the volume of the solvent is set to be 3 mL. As shown in Figure S6 (Supporting Information), Sul_2-Sor_3-Eug_5 is soluble in most solvents except some extremely polar or extremely nonpolar solvents such as H_2O and *n*-Hexane, toluene. It is surmised that the good solubility is owing to the complete consummation of sulfur, the small molecular weight as well as the structure of the polymer material which is branched or crosslinked with low crosslinking density.

Moreover, biological experiments were conducted to determine the toxicity of samples for practical applications. In

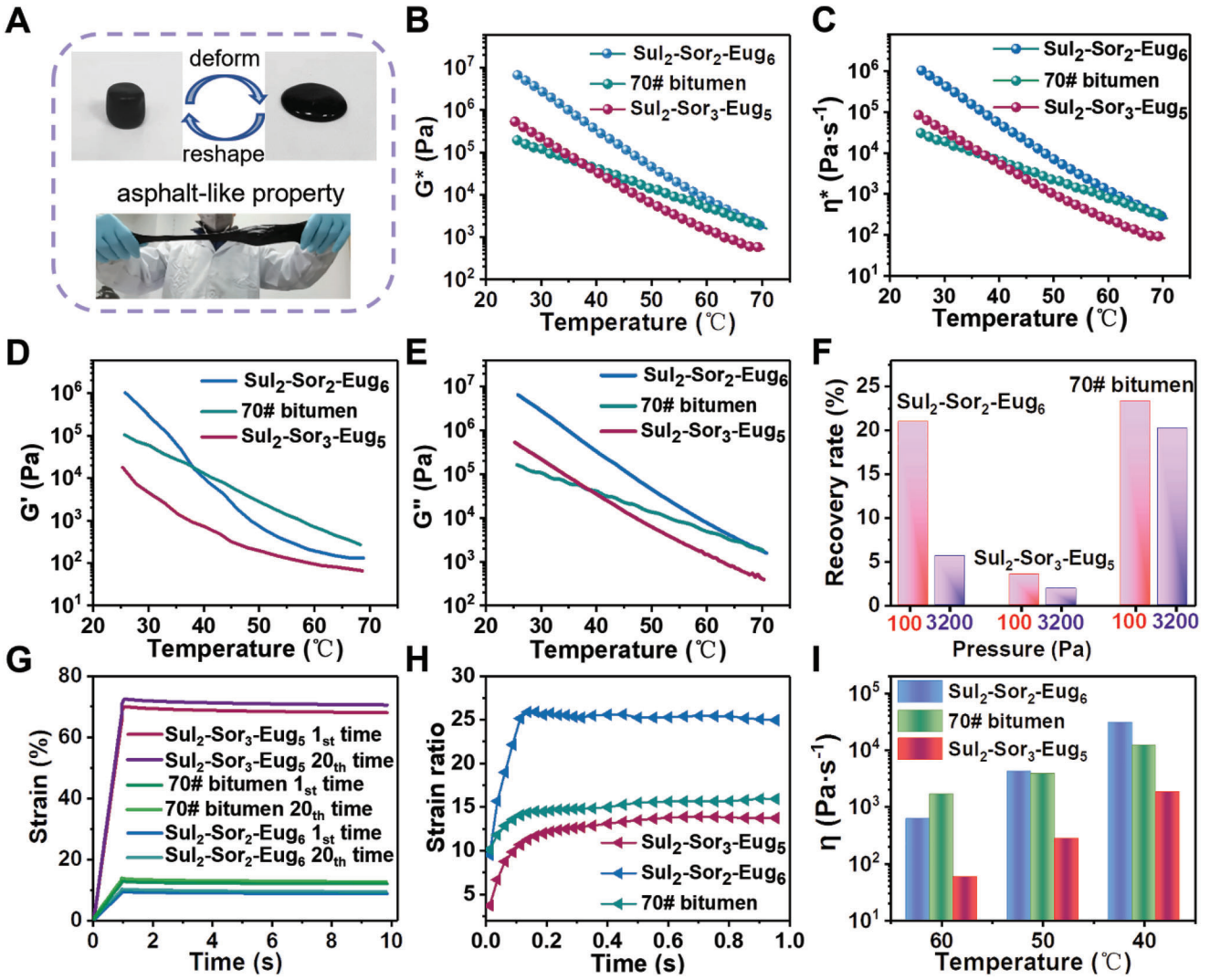

Figure 2. Comparison of rheological properties and creep properties of bitumen and Sul-Sor-Eug. A) Bitumen-like phenomenon of Sul_2-Sor_3-Eug_5. B) Complex moduli, C) complex viscosity, D) storage modulus, E) loss modulus of 70# bitumen, Sul_2-Sor_2-Eug_6, and Sul_2-Sor_3-Eug_5 at a frequency of 1 Hz, strain of 1%. F) Recovery rate of Sul_2-Sor_3-Eug_5, Sul_2-Sor_2-Eug_6, and 70# bitumen at 40 °C. G) Creep recovery curve of Sul_2-Sor_2-Eug_6, Sul_2-Sor_2-Eug_6, and 70# bitumen at 60 °C, 100 Pa. H) Strain ratio at 60 and 40 °C of Sul_2-Sor_2-Eug_6, Sul_2-Sor_2-Eug_6, and 70# bitumen. I) The viscosity of Sul_2-Sor_3-Eug_5, Sul_2-Sor_2-Eug_6, and 70# bitumen at 40, 50, and 60 °C.

the acute inhalation experiment, the mice did not show any symptoms of poisoning and death of poisoning within fourteen days of infection, while no abnormal changes in the weight tracking of male and female mice were observed, even though the acute inhalation value of the sample for mice (LC50) was quite high (up to 6634.4 mg cm^{-3}) (Figure S7, Supporting Information). As shown in Tables S3 and S4 (Supporting Information), the fish stayed alive in the leaching solution at a soaking concentration of 100 mg mL^{-1} for 72 h and the amount of dissolved oxygen in the experimental group only decreased slightly. There was basically no difference in pH compared to the control group. We also conducted a rabbit skin irritation experiment to evaluate the skin irritation of people who may come into contact with the sample. As shown in Table S5 (Supporting Information), no abnormalities were seen in the rabbit skin within 72 h of contact with the sample. Overall, the sample is non-toxic to the organism and does not have a significant impact on water quality in the short term which is advantageous to bitumen and favorable for practical application.

2.2. Bitumen-Like Property

The as-prepared Sul_2-Sor_2-Eug_6 and Sul_2-Sor_3-Eug_5 are pitch-black and show significant creep deformation although they can be processed into a cylinder shape (**Figure 2**A, taking Sul_2-Sor_2-Eug_6 as an example). Moreover, a plate sample can be highly stretchable if it is stretched slowly, but it will break upon quick stretching (Figure 2A, Movie S1, Supporting Information). This phenomenon reminds us of the similarity between these polymers and bitumen. Therefore, we systematically compared their properties with those of the commonest 70# bitumen

which is a product of crude oil processing. The physical properties and chemical compositions of 70# bitumen are listed in Table S6 (Supporting Information).[49] As shown in Figure 2B, the complex modulus of Sul_2-Sor_2-Eug_6 is the largest in the low-temperature region, which indicates that the ability of Sul_2-Sor_2-Eug_6 to resist deformation is the strongest. As the temperature rises, the complex modulus of the three substances decreases and the complex modulus of Sul_2-Sor_2-Eug_6 changes fastest, indicating that it has the best temperature-sensing characteristics. The softening points are 40, 38, and 52 °C for 70# bitumen, Sul_2-Sor_3-Eug_5, and Sul_2-Sor_2-Eug_6, respectively. It is consistent with the results of dynamic complex modulus. The complex viscosity decreases exponentially with the increase in temperature, which is also consistent with the changing trend of complex modulus. It can be seen from Figure 2C that Sul_2-Sor_2-Eug_6 has stronger resistance to shear deformation compared to 70# bitumen and Sul_2-Sor_3-Eug_5 in the temperature range of 25–70 °C. The storage modulus and loss modulus both decrease with the increase of temperature as shown in Figures 2D,E. The decreasing trend of storage modulus is greater, indicating that the proportion of viscous components increases with the increase of temperature and the ability to resist deformation decreases. Furthermore, phase angle decreases as temperature rises (Figure S8, Supporting Information), implying that viscosity increases as temperature rises, which is consistent with the results of storage modulus and loss modulus.

We conducted multiple stress (100 and 3200 Pa) creep recovery tests (MSCR) to better compare the high-temperature stability of 70# bitumen and bitumen-like polymers. The main evaluation indicators are deformation recovery rate R and irrecoverable creep compliance J_{nr}, which are closely related to the high-temperature rutting performance of asphalt pavement. The changes in strain and creep compliance of Sul_2-Sor_2-Eug_6 at 40 and 60 °C are shown in Figure S9A,B (Supporting Information), respectively. It could be seen that the strain is higher while the creep compliance is lower under 3200 Pa as compared to 100 Pa at the same temperature. The strain and the creep compliance increased due to the decrease of viscosity at higher temperatures, thus the resistance to deformation is weakened at 60 °C as compared to 40 °C under the same pressure. Sul_2-Sor_3-Eug_5 and 70# bitumen exhibited a similar trend (Figures S10,S11, Supporting Information). Under the same conditions, the strain and creep compliance of Sul_2-Sor_3-Eug_5 are smaller, indicating that the high-temperature resistance to rutting of Sul_2-Sor_3-Eug_5 is stronger. We also compared the strain recovery in the first and twentieth creep recovery cycles. As shown in Figure 2F and Figure S12 (Supporting Information), Sul_2-Sor_3-Eug_5 shows the lowest recovery efficiency. Although the recovery efficiency of Sul_2-Sor_2-Eug_6 is a little bit lower than 70# bitumen, Sul_2-Sor_2-Eug_6 still shows the lowest irrecoverable strain (Figure 2G). Detailed information is shown in Tables S7–S10 (Supporting Information). The strain ratio of the three samples at 60 and 40 °C under 100 Pa were also analyzed. As shown in Figure 2H, Sul_2-Sor_2-Eug_6 shows the highest strain ratio, indicating that it has the best temperature sensitivity which benefits to on-site construction.

The basic physical and chemical properties of bitumen-like polymers and bitumen were also compared. Figure 2I illustrates the viscosity of three samples at different temperatures. Sul_2-Sor_2-Eug_6 shows the highest viscosity at 40 °C while 70# bitumen shows the highest viscosity at 60 °C among the three samples, indicating that Sul_2-Sor_2-Eug_6 has the best temperature sensitivity which is consistent with the rheological test. A GPC test (Gel Permeation Chromatography) was also conducted. As shown in Figures S13 and S14 and Table S11 (Supporting Information), the number average molecular weights of the three samples are all ≈1000. The densities of the sulfur-containing polymers are slightly higher than that of bitumen (Table S12, Supporting Information). The contact angles of Sul_2-Sor_2-Eug_6, Sul_2-Sor_3-Eug_5 and 70# bitumen are 89.15°/ 90.11°, 88.96°/ 85.26° and 104.74°/ 105.32°, respectively (Figure S15, Supporting Information). On this basis, the stability of the sample in an aqueous environment was also tested. As shown in Figure S16 (Supporting Information), upon soaking the samples in water for about three months, the solution has no obvious discoloration. We have made a statistical comparison of the mass before and after immersion, which shows that the sample is very stable in water (Figure S17, Supporting Information). As shown in Figure S18 (Supporting Information), the TGA test of Sul_2-Sor_2-Eug_6 and 70# bitumen shows that both samples were stable from 30 to 200 °C. Moreover, considering that the bitumen-like materials via inverse vulcanization may suffer the biteback of the polysulfur chain and further sulfur crystallization during the duration of storage at ambient temperature. Rheology tests were conducted to evaluate the anti-aging properties of Sul_2-Sor_3-Eug_5. As shown in Figure S19 (Supporting Information), there was no obvious increase in loss modulus and storage modulus after the sample was left for 12 months at ambient temperature. In addition, the DSC curve proved that sulfur crystallization did not appear even though Sul_2-Sor_3-Eug_5 had been left for 12 months indicating that Sul_2-Sor_3-Eug_5 has superior anti-aging properties at ambient temperature (Figure S20, Supporting Information).

2.3. Shear Stiffening and Self-Healing Performance

As shown in **Figure 3**A, there is an obvious solid-like landing rebound phenomenon after the ball-shaped Sul_2-Sor_3-Eug_5 polymer dropped. When the strip of Sul_2-Sor_3-Eug_5 was quickly thrown to the table, it instantly broke into several segments (Figure 3B, Movie S2, Supporting Information). Moreover, when the pie-shaped Sul_2-Sor_3-Eug_5 was hit with a blunt tool, cracks would appear instantaneously (Figure S21, Supporting Information). As shown in Movie S1 (Supporting Information), it showed a sticky behavior when the volunteer pulled it by hands. However, when it was hit quickly by the volunteer, it immediately became hard and brittle. All these phenomena indicate the existence of shear stiffening performance.[50–55] We performed rheological tests to quantitatively characterize this solid–liquid transition behavior. As shown in Figure 3C, the storage modulus of Sul_2-Sor_3-Eug_5 is only 10^2 Pa in the low-frequency region, showing a completely viscous behavior. However, it increased rapidly as the external strain rates increased to the critical value. In this case, the storage modulus of Sul_2-Sor_3-Eug_5 reached as high as 10^8 Pa. Figure 3D demonstrates the viscoelastic transition process. G′ was much smaller than G″ in the low-frequency region. As the frequency increased, the material exhibited obvious shear stiffening behavior accompanied by a

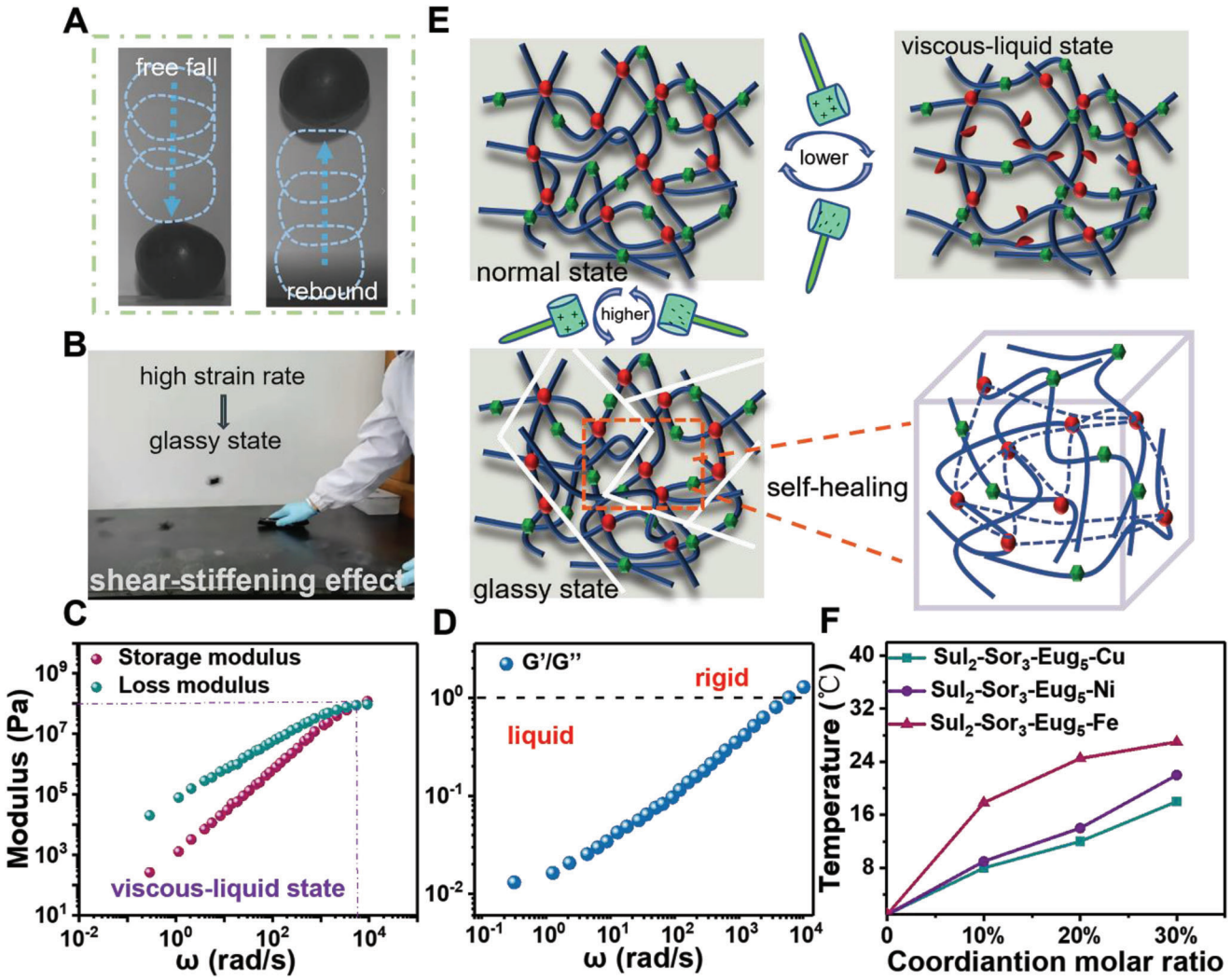

Figure 3. Shear stiffening effect and mechanism. A) Landing rebound phenomenon of Sul_2-Sor_3-Eug_5. B) Photograph of strip-shaped Sul_2-Sor_3-Eug_5 being hit. C) Master curves at a reference temperature of 25 °C, prepared by the time-temperature superposition treatment of storage modulus (G′) and loss modulus (G″) values obtained at 0, 5, 10, 20, 25, 30, and 40 °C, in frequency-dispersion tests [frequency (ω) = 628 to (6.28×10^{-3}) rad s^{-1}] at an applied strain of 0.1% or 1%. D) The ratio of G′ and G″ values obtained at 0, 5, 10, 20, 25, 30, and 40 °C, in frequency-dispersion tests [frequency (ω) = 628 to (6.28×10^{-1}) rad s^{-1}] at an applied strain of 0.1% or 1%. E) The mechanism of shear stiffening effect and self-healing performance. F) The change of soft-rigid transition point after crosslinking by coordination bonds.

rapid increase in storage modulus, after reaching the cross-point of G′ and G″.[56,57] A possible mechanism for this phenomenon was proposed. As shown in Figure 3E, there are both flexible polymer backbone and rigid aromatic domains in the polymer, both of which contribute to the soft-hard conversion behavior. The flexible polymer backbone ensures low glass transition temperature and fluidity at room temperature. The rigid aromatic domains ensure that the movement of the molecular chain can be restricted when subjected to high-speed impact, thus the polymer can be instantly hardened by the yield of the molecular chain. When the strain rate is lower, the loading time is much longer than the relaxation time of the crosslinking interactions (here is the hydrogen bonds). As a result, the time is enough for the hydrogen bonds to dissociate and the molecular chains to disentangle, thus the polymer exhibits plasticity and fluidity and is in a viscous-liquid state. Due to the same reason, the polymer exhibits superior self-healing properties. Samples after cutting can flow and adhere together further recovering the mechanical strength within 30 min at room temperature as demonstrated in Movie S3 and Figure S22 (Supporting Information). However, when the strain rate is lower, the loading time is not long enough for the hydrogen bonds to dissociate and the molecular chains to disentangle. The internal structure of the polymer seems to be "frozen" from a microscopic point of view. At this time, it is hard and brittle, thus easy to be broken.

On this basis, we conducted a systematic exploration of the factors that may affect the shear stiffening behavior. The indispensability of sulfur through comparative experiments was first proved. When only sorbic acid and eugenol react under the same conditions, the product is a mixture of red and white solid which is judged to be unreacted (Figure S23, Supporting Information). If ethyl sorbate is used to replace sorbic acid or

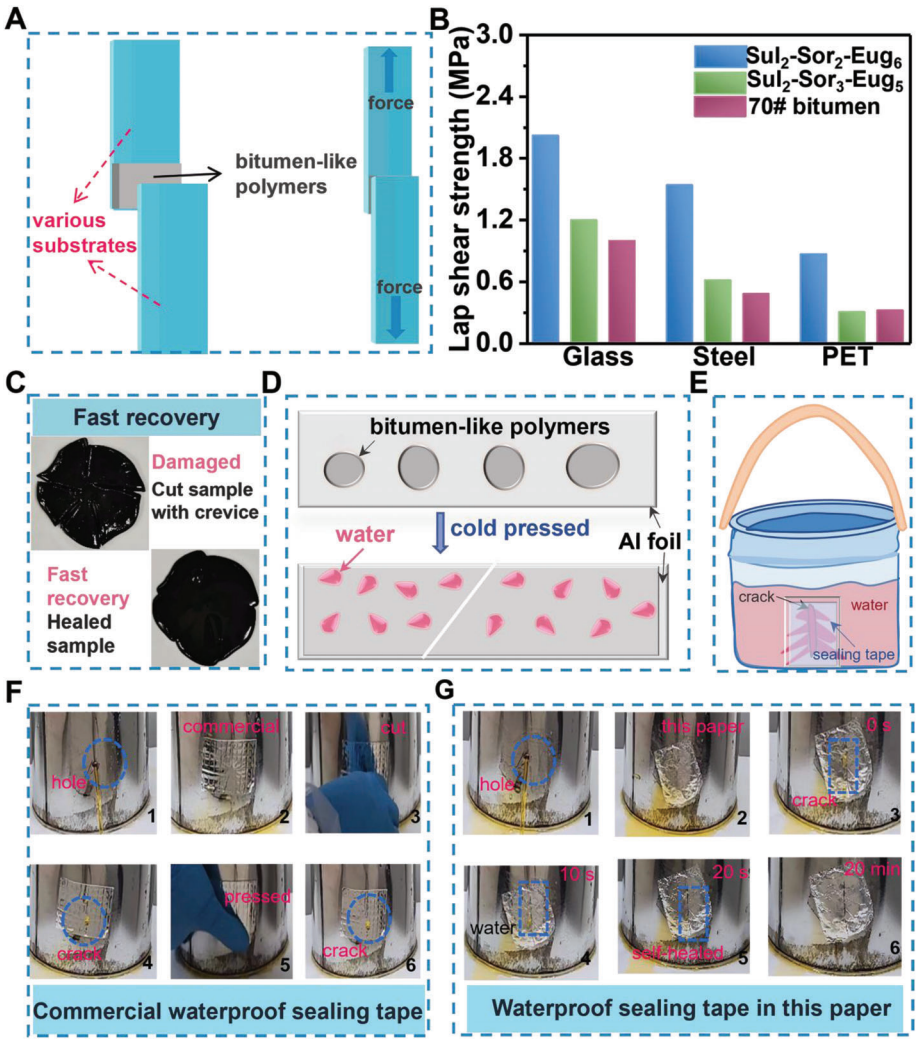

Figure 4. Applications of Sul-Sor-Eug for waterproof-sealing tape. A) Schematic representation of standard lap shear test geometry. B) The corresponding lap shear strength of Sul_2-Sor_3-Eug_5, Sul_2-Sor_2-Eug_6, and 70# bitumen to Glass, steel, and PET. C) Fast recovery ability of Sul_2-Sor_2-Eug_6. D) The preparation process of waterproof sealing tape. E) Schematic diagram of the use of waterproof sealing tape. F) Self-healing performance of commercial sealing tape with compression after being damaged. G) Self-healing performance of the sealing tape in this paper without compression after being damaged.

4-allyl-1,2-dimethoxybenzene to replace eugenol, the strength of the material will be significantly reduced (Figure S24, Supporting Information), indicating that hydrogen bonding has a significant effect on strength. The modulus of the material decreases with the decrease of aromatic ring content and the increase of sulfur content (Figure S25, Supporting Information). Overall, the initial modulus is determined by the crosslinking bonds and hard segment, and the frequency of the soft and rigid conversion points is determined by the crosslinking bonds. Inspired by this, we use another dynamic bond metal coordination bond to adjust the soft-rigid transition temperature of the material. Considering the coordination strength of different metal ions, the metal salts were chosen to be $FeCl_3{\cdot}6H_2O$, $NiCl_2{\cdot}6H_2O$, and $CuCl_2{\cdot}2H_2O$. As shown in Figure 3F, the soft-rigid transition temperatures of the coordination polymers are higher than that of Sul_2-Sor_3-Eug_5 and Sul_2-Sor_2-Eug_6 and can be effectively tuned by adjusting the type and coordination ratio of the metal ions. Therefore, the coordination materials could fit higher working temperatures in which Sul_2-Sor_3-Eug_5 and Sul_2-Sor_2-Eug_6 may be in a liquid state and thus unfavorable for self-supporting or shear-stiffening. The excellent tunability and adaptability of these materials are of great significance to broaden the working environment temperature of the material.

2.4. Various Applications

Since bitumen is useful in widespread fields, we expect that the bitumen-like polymers obtained in this work also have various applications. First, we investigated their application in self-healing adhesives and sealants. The preparation process of the lap shear adhesion tests is shown in **Figure 4**A. As illustrated in Figure 4B, Sul_2-Sor_2-Eug_6 shows the highest adhesive strength to various substrates which is probably related to the hydrogen bonding

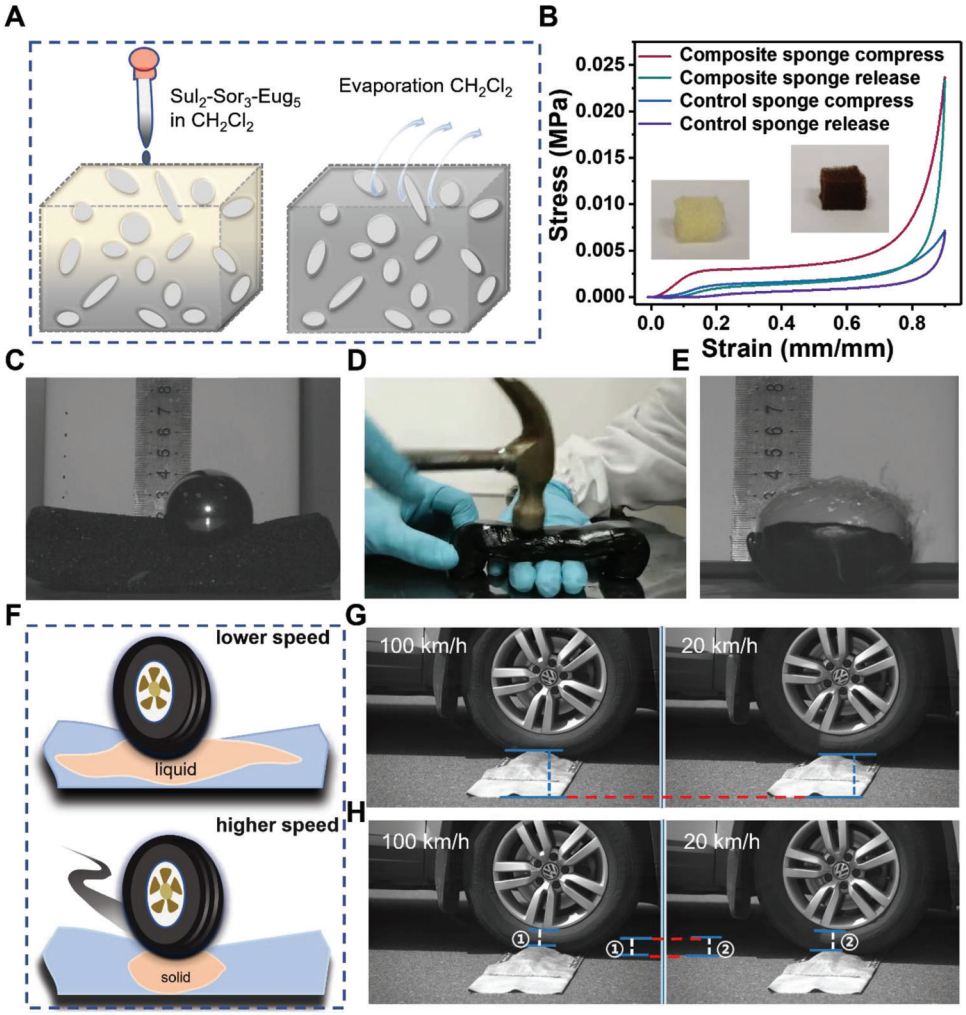

Figure 5. Applications of Sul-Sor-Eug for impact resistance and non-Newtonian speed bump. A) The preparation process of impact-resistant sponge composite. B) Cyclic compress-release curves of blank sponge and 20% wt Sul_2-Sor_3-Eug_5 soaked composite sponge. C) Sul_2-Sor_3-Eug_5 soaked composite sponge used as shock absorbing. D) Sul_2-Sor_3-Eug_5 used as arch protection. E) Sul_2-Sor_3-Eug_5 is used as a protective shell for eggs. F) The work principle of Sul_2-Sor_2-Eug_6 filling speed pumps at higher speed and lower speed. G) Difference of the height of the speed pump at different speeds (100 and 20 km h^{-1}) recorded by high-speed cameras when wheels pass over the speed pump. H) Difference of the distance from the outer edge of the wheel to the hub of speed pump at different speeds (100 and 20 km h^{-1}) recorded by high-speed cameras when wheels pass over the speed pump.

between Sul_2-Sor_2-Eug_6 and the adhered substates. The corresponding average lap shear strength of Sul_2-Sor_2-Eug_6 to different substrates was tested to be 2.02 MPa to Glass, 1.53 MPa to steel, and 0.30 MPa to PET, respectively. We also performed the water absorption experiments to explore the sealing property of Sul_2-So_2-Eug_6. The discolored silica gel without sealant absorbs water more obviously (Figure S26, Supporting Information). Peel strength is also one of the most important values for the use of sealants, therefore, peel tests of Sul_2-Sor_2-Eug_6 were conducted. As shown in Figure S27 (Supporting Information), the peel strength of Sul_2-Sor_2-Eug_6 is 151.80 ± 3.81 N m^{-1}, indicating that the sealant is easy to be peeled off. Moreover, Sul_2-Sor_2-Eug_6 cut with crevice could recover after 30 min demonstrating fast recovery ability (Figure 4C). Due to its excellent adhesion and sealing ability, a self-healing waterproofing sealing tape was prepared. The preparation process of waterproof sealing tape is shown in Figure 4D. The sealing tape can effectively adhere to the surface of the broken container and prevent the internal liquid from leaking (Figure 4E). Furthermore, the self-healing performance of our waterproof sealing tapes was compared with the commercial one. As shown in Figure 4F, the commercial sealing tape could prevent the internal liquid from leaking. However, it can not repair after cutting, even though we have compressed it to facilitate the process of repair. Instead, the waterproof sealing tape in this work could achieve fast self-healing in 20 s without any external pressure after cutting (Figure 4G, Movie S4, Supporting Information).

As the bitumen-like polymers show excellent shear stiffening effects, we further investigated its application as intelligent protective materials. As shown in **Figure 5**A, the sponge was soaked with Sul_2-Sor_3-Eug_5 by the "dip and dry" method. The resulting composite sponge shows higher energy dissipation density as compared to the pristine one (Figure 5B). The impact energy could be absorbed when a 500 g steel ball fell on

the composite sponge, therefore, the ball did not bounce back (Figure 5C, Movie S5, Supporting Information). As shown in Figure 5D, Sul_2-Sor_3-Eug_5 was squeezed into an arched bridge to protect the hand. When it was hit with a hammer, it quickly hardened and produced a loud sound similar to hitting a solid, but the hand had no feeling of hitting at all (Movie S6, Supporting Information). It could also be utilized to protect fragile items. For example, the egg remained intact after falling from a high place after wrapping a layer of Sul_2-Sor_3-Eug_5 on the outside (Figure 5E, Movie S7, Supporting Information). A speed bump was also manufactured benefiting from the shear stiffening property of Sul_2-Sor_2-Eug_6 (Figure S28, Supporting Information). As shown in Figure 5F, Sul_2-Sor_2-Eug_6 inside the speed bump is viscous when the vehicles pass at a lower speed (20 km h^{-1}), therefore it will deform significantly upon compression and thus avoid jolt sensation. Instead, it will exhibit solid-like properties at a higher speed (100 km h^{-1}). Therefore, people inside the car will feel an apparent jolt sensation. These differences can be manifested by the different heights of the speed bump and different distances from the outer edge of the wheel to the hub under different speeds (Figure 5G,H; Figure S29, Supporting Information). It can also be seen that the speed bump would leave a certain degree of rut marks at lower speeds, but it could maintain shape integrity at higher speeds (Figure S30, Movie S8, Supporting Information). Such new speed bumps can not only achieve the deceleration effect in high-speed driving, enhance driving comfortability in low-speed driving compared with traditional speed bumps, but also avoid problems caused by non-Newtonian fluid speed bumps such as phase separation, solid deposition, and liquid leaking. It is noteworthy that although the polymer will break upon impact, it can self-heal quickly and thus can maintain its function upon damage.

Sealants have been widely used in industrial applications such as pipes and guttering, flooring, glazing, and roofing.[58] Among various sealants for different applications, water-proof sealant is the most useful one as they can not only close gaps in water pipes and hold the materials together but also can keep out the water to protect water-insensitive surfaces in construction and home projects.[58,59] According to the statistical data, the global waterproof adhesive & sealant market size was estimated at USD 23.4 billion in 2022 and expected to reach USD 31.3 billion in 2027, at a compound annual growth rate (CAGR) 6.69%.[60] On the other hand, speed bumps have been extensively used to reduce traffic speed on local streets. Due to the increasing focus of governments all over the world on road safety, the demand for traffic speed bumps is expected to skyrocket in the near future. Providing that the bitumen-like polymers obtained in this work are useful in water-proof sealants and traffic speed bumps, we believe that a huge amount of waste sulfur will be consumed while the unsustainability of bitumen will be significantly alleviated.

3. Conclusion

In summary, we obtained bitumen-like polymers from sulfur, sorbic acid, and eugenol through an inverse vulcanization reaction. The sulfur-containing polymer not only shows properties similar to bitumen but also has shear stiffening and self-healing performance. We have proved that Sul_2-Sor_2-Eug_6 has better resistance to permanent deformation and high-temperature resistance to rutting as compared to 70# bitumen. Moreover, bitumen-like polymers have been used in waterproof sealing tape with self-healing ability which can repair without any external pressure after being cut. Furthermore, the polymer can also be used in smart protective materials and shock absorption devices due to its shear-hardening characteristics, which not only broadens the source of shear-hardened materials but also provides more possibilities for the development of next-generation smart protective materials. Besides, it also has been utilized as the content to prepare non-Newtonian speed bumps which can ensure both comfortability at lower speeds and the deceleration effect at higher speeds. Overall, we provide a new way of turning excessive sulfur into multifunctional products and overcoming the unsustainable problem of bitumen, with the advantages including easy massed-fabrication, non-toxicity, extremely low cost (≈2 cents per gram), and environment friendliness.

4. Experimental Section

Materials Synthesis: Sul_2-Sor_2-Eug_3 was synthesized through inverse vulcanization with sorbic acid, eugenol, and sulfur as starting materials. The total mass of raw materials was set to 10 g, and the weight percentages of sulfur (99%; Sigma-Aldrich), sorbic acid (99%; Aladdin), and eugenol (99%; Aladdin) were 20, 20, and 60 wt. %, respectively. All the raw materials were added to the pressure tube equipped with a magnetic stir bar, and then the catalyst Zn $(DTC)_2$ (99%; Sigma-Aldrich) (100 mg) was added. After the reaction flask was evacuated and replaced with nitrogen three times, it was placed in an oil bath for reaction at 160 °C for 4 h. After the reaction, the whole mixture cooled down for 2 min followed by ≈20 h curing at 120 °C in the oven. Other Sul_x-Sor_y-Eug_z polymers were prepared similarly but with different weight percentages of starting materials. For the soaking sponge with Sul_2-Sor_3-Eug_5, 2.5 g of Sul_2-Sor_3-Eug_5 was dissolved in 30 mL of dichloromethane (AR; Aladdin). A cuboid sponge (5 g) was repeatedly soaked in the solution and placed in a ventilated place to air dry during the period. For coordinating Sul_2-Sor_2-Eug_6 with metal ions, a certain amount of Sul_2-Sor_2-Eug_6 is weighed and dissolved in a methanol solution. Different metal salts were weighed according to the coordination ratio and dissolved in deionized water. A constant pressure-dropping funnel was used to slowly drop the metal into the methanol solution. Then the mixture was stirred at room temperature for 4 hours. Methanol was removed by rotary evaporation at 50 °C, and vacuum dry process at 80 °C for 24 h.

Characterization of the Synthesized Bitumen-Like Polymers: Solution NMR was recorded in deuterated chloroform using a Bruker Advance DRX (400 MHz) spectrometer. DMSO-*d6* was used as the solvent. Elemental analysis was conducted by Elementar UNICUBE. FT-IR was carried out using Vertex 70 Fourier Transform Infrared Spectrometer, from 400 to 4000 cm^{-1}. DSC was carried out using Q2000 DSC (TA instruments). The method was a heat/cool/heat for three cycles at a heating/cooling rate of 10 °C min^{-1} and ranging from −50 to 80 °C. The second heating curves were recorded and analyzed. Crystal fraction of polymer was detected using a PANalytical X'Pert PRO diffractometer with Cu-$K_{\alpha 1+2}$ radiation, operating in transmission geometry. The thermal stability of sulfur-polymers was conducted using a TA Instruments Q500 under nitrogen from 30 to 600 °C at a heating rate of 20 °C min^{-1}. The molecular weight was measured by using Viscotek TDA302 GPC (THF). All the concentrations of samples were prepared as 5 mg ml^{-1}. Toxicity tests were conducted by Ningbo Customs District P. R. China.

Characterization of Rheological and Mechanical Properties: Rheological behavior was evaluated by using the DHR-2 Rheometer (TA Instruments). The temperature ramp test was conducted at temperatures ranging from 25 to 70 °C with 5 °C increments and under a frequency of 1 Hz, strain of

1% with 20 mm parallel plates. The viscosity was tested at temperatures ranging from 40 to 60 °C with 5 °C increments and under a shear rate of 1 s^{-1}. The uniaxial tensile test was conducted by an Instron 3343 with molded samples. The tensile speed was set at 150 mm^{-1}. Three samples were prepared for each tensile experiment. For MSCR, the specimens were subjected to creep and recovery experiments at 40 and 60 °C with two constant stresses (100 and 3200 Pa) respectively. After the stress loading lasted for 1 s, the zero stress recovered for 9 s. The experiment experienced 30 creeps and cycles. Twenty cycles were performed under 100 Pa stress and 10 cycles under 3200 Pa stress, for a total of 30 cycles. There was no relaxation time and stress change between creep and recovery cycles.

Lap Shear Adhesion Test: All the substrates were first polished with sandpaper and then washed with soap water and acetone. The adherents referring to Sul_2-Sor_3-Eug_5, Sul_2-Sor_2-Eug_6, and 70# bitumen were spread on the substrate, and the other substrate was overlapped on it. The two substrates were hot pressed at 70 °C under 0.1 MPa for 20 min to obtain a lap shear sample with an overlapped area of 10 mm × 10 mm. The lap shear strength was measured by an Instron 3343 instrument. A crosshead speed of 20 mm min^{-1} was employed in all cases. Lap shear adhesion was defined as the maximum force (in newtons) of the adhesive joint obtained from the lap shear test divided by the overlap area (in square millimeters) of adhesives.[61,62]

$$\text{Lap shear strength} = \frac{\text{Force } (N)}{\text{Adhesive area } (mm^2)} \quad (1)$$

Peel Test: The peel test was configured with a 180° peel angle. In order to ensure the accuracy of the results, the experiment was carried out in parallel with 5 sets. The steel plate was taped at the bottom and the 125 µm thick PET was placed on top, a 2 mm thick sealant layer was sandwiched between them. The width and length of the sealant layer was 15 and 150 mm, respectively. The test speed was 300 mm min^{-1}. $\sigma_{180°}$, F and B correspond to the peel strength, peel force, and specimen width, respectively.

$$\sigma_{180°} = \frac{F}{B} \quad (2)$$

Stability Test: The stability of the bitumen-like polymers in the aqueous environment was tested by soaking a certain quality sample in deionized water. After 3 months of soaking, the samples were removed and weighed after drying thoroughly at 80 °C under vacuum.

Supporting Information

Supporting Information is available from the Wiley Online Library or from the author.

Acknowledgements

K.X.H. and P.C.Z. contributed equally to this work. This work was supported by the National Natural Science Foundation of China (Grant No. 22271139 and 21771100) and the Natural Science Foundation of Jiangsu Province (Grant No. BK20210440). The authors would like to thank Prof. Bo-Xing Hu for the help in the measurement of softening points and Prof. Zhi-Bing Zhang, Guo-Qiang Yang, and Qiang Li for the support of high-speed camera devices and technology.

Conflict of Interest

The authors declare no conflict of interest.

Data Availability Statement

The data that support the findings of this study are available from the corresponding author upon reasonable request.

Keywords

multifunctional, polymers, self-healing, shear stiffening, sulfur

Received: June 17, 2023
Revised: July 29, 2023
Published online:

[1] E. J. Barth, *Nature* **1964**, *4934*, 739.
[2] J. F. Black, *Science* **1963**, *139*, 226.
[3] A. Moriyoshi, I. Fukai, M. Takeuchi, *Nature* **1990**, *344*, 230.
[4] O. Andersson, *Nature* **1966**, *211*, 402.
[5] L. Xu, H. Ni, Y. Zhang, D. Sun, Y. Zheng, M. Hu, *J. Cleaner Prod.* **2022**, *376*, 134119.
[6] W. Yang, R. Li, B. Jiang, T. Wang, L. Hou, Z. Li, Z. Liu, F. Yang, Y. Li, *Carbon* **2020**, *166*, 218.
[7] H. Yao, J. Liu, M. Xu, J. Ji, Q. Dai, Z. You, *Adv. Colloid Interface Sci.* **2022**, *299*, 102565.
[8] C. Richardson, *Nature* **1905**, *72*, 316.
[9] I. R. Segundo, E. Freitas, V. T. F. C. Branco, S. L. Jr, M. F. C. Carneiro, *Renewable Sustainable Energy Rev.* **2021**, *151*, 111552.
[10] C. Ashworth, *Nat. Rev. Earth Environ.* **2020**, *1*, 497.
[11] S. Mo, Y. Wang, F. Xiong, C. Ai, *J. Hazard. Mater.* **2019**, *371*, 342.
[12] M. Mousavi, E. H. Fini, *J. Cleaner Prod.* **2022**, *344*, 131067.
[13] X. Yang, G. Wang, H. Rong, Y. Meng, X. Liu, Y. LIU, C. Peng, *J. Cleaner Prod.* **2022**, *347*, 131240.
[14] J. Liggio, S.-M. Li, K. Hayden, Y. M. Taha, C. Stroud, A. Darlington, B. D. Drollete, M. Gordon, P. Lee, P. Liu, A. Leithead, S. G. Moussa, D. Wang, J. O'Brien, R. L. Mittermeier, J. R. Brook, G. Lu, R. M. Staebler, Y. Han, T. W. Tokarek, H. D. Osthoff, P. A. Makar, J. Zhang, D. L. Plata, D. R. Gentner, *Nature* **2016**, *534*, 91.
[15] L. P. Thives, E. Ghisi, *Renewable Sustainable Energy Rev.* **2017**, *72*, 473.
[16] M. Vila-Cortavitarte, P. Lastra-González, M. Á. Calzada-Pérez, I. Indacoechea-Vega, *J. Cleaner Prod.* **2018**, *170*, 1279.
[17] X. Hu, M. Gholizadeh, *Renewable Sustainable Energy Rev.* **2020**, *134*, 110124.
[18] S. Bressi, M. Primavera, J. Santos, *Resour., Conserv. Recycl.* **2022**, *180*, 106160.
[19] K. Schwettmann, N. Nytus, S. Weigel, M. Radenberg, D. Stephan, *Resour. Conserv. Recycl.* **2023**, *190*, 106776.
[20] R. J. Angelici, *Acc. Chem. Res.* **1988**, *21*, 387.
[21] T. Rauchfuss, *Nat. Chem.* **2011**, *3*, 648.
[22] E. Stokstad, *Science* **2018**, *362*, 146.
[23] D. H. Kim, W. Jang, K. Choi, J. S. Choi, J. S. Choi, J. Pyun, J. Lim, K. Char, S. G. Im, *Sci. Adv.* **2020**, *6*, eabb5320.
[24] J. E. Mark, *Prog. Polym. Sci.* **2003**, *28*, 1205.
[25] M. Wang, Z. Bai, T. Yang, C. Nie, X. Xu, Y. Wang, J. Yang, S. Dou, N. Wang, *Adv. Energy Mater.* **2022**, *12*, 2201585.
[26] H. Wang, Y. Xiong, S. V. Kershaw, T. Li, Y. Wang, Y. Zhai, A. L. Rogach, *Angew. Chem., Int. Ed.* **2019**, *58*, 7040.
[27] C. Jia, F. Zhang, N. Zhang, Q. Li, X. He, J. Sun, R. Jiang, Z. Lei, Z. H. Liu, *ACS Nano* **2023**, *17*, 1713.
[28] Y. Wang, Y. Zhao, J. Wu, M. Li, J. Tan, W. Fu, H. Tang, P. Zhang, *Nano Lett.* **2021**, *21*, 9433.
[29] J. Liu, X. He, B. Wu, *Acc. Chem. Res.* **2021**, *54*, 4215.
[30] H. Jin, Y. Sun, Z. Sun, M. Yang, R. Gui, *Coordin. Chem. Rev.* **2021**, *438*, 213913.
[31] W. J. Chung, J. J. Griebel, E. T. Kim, H. Yoon, A. G. Simmonds, H. J. Ji, P. T. Dirlam, R. S. Glass, J. J. Wie, N. A. Nguyen, B. W. Guralnick, J. Park, A. Somogyi, P. Theato, M. E. Mackay, Y. E. Sung, K. Char, J. Pyun, *Nat. Chem.* **2013**, *5*, 518.

[32] C. Garrigue, P. Vincent, *Sulfur /Asphalt Binders for Road Construction, Advances in Chemistry*, American Chemical Society, Washington, DC, **1975**.
[33] N. Xu, H. Wang, H. Wang, M. Kazemi, E. Fini, *J. Cleaner Prod.* **2023**, *385*, 135427.
[34] F. Pahlavan, E. H. Fini, *Resour., Conserv. Recycl.* **2022**, *180*, 106184.
[35] W. Huang, *Sci. Bull.* **2003**, *48*, 2391.
[36] A. Eisenberg, A. V. Tobolsky, *J. Polym. Sci.* **1960**, *46*, 19.
[37] J. Jia, J. Liu, Z. Q. Wang, T. Liu, P. Yan, X. Q. Gong, C. Zhao, L. Chen, C. Miao, W. Zhao, S. Cai, X. C. Wang, A. I. Copper, X. Wu, T. Hasell, Z. J. Quan, *Nat. Chem.* **2022**, *14*, 1249.
[38] L. B. Blight, B. R. Currell, B. J. Nash, R. T. M. Scott, C. Stillo, *Br. Polym. J.* **1980**, *12*, 5.
[39] A. Hoefling, D. T. Nguyen, Y. J. Lee, S. W. Song, P. Theato, *Mater. Chem. Front.* **2017**, *1*, 1818.
[40] X. Ji, K. T. Lee, L. F. Nazar, *Nat. Mater.* **2009**, *8*, 500.
[41] M. S. Brewer, *Compr. Rev. Food Sci. Food Saf.* **2011**, *10*, 221.
[42] D. J. Parker, S. Y. Chong, T. Hasell, *RSC Adv.* **2018**, *8*, 27892.
[43] M. J. H. Worthington, R. L. Kucera, J. M. Chalker, *Green Chem.* **2017**, *19*, 2748.
[44] N. Amornruk, M. Siranart, P. Sittiwattanawong, P. Kueanjinda, S. Loplumlert, J. Wongpiyabovorn, *J. Am. Acad. Dermatol.* **2022**, *87*, 1042.
[45] D. K. Salunkhe, *Nature* **1956**, *178*, 1187.
[46] X. Wu, J. A. Smith, S. Petcher, B. Zhang, D. J. Parker, J. M. Griffin, T. Hasell, *Nat. Commun.* **2019**, *10*, 647.
[47] J. J. Griebel, S. Namnabat, E. T. Kim, R. Himmelhuber, D. H. Moronta, W. J. Chung, W. A. G. Simmonds, K. J. Kim, J. Laan, N. A. Nguyen, E. L. Dereniak, M. E. Mackay, K. Char, R. S. Glass, R. A. Norwood, J. Pyun, *Adv. Mater.* **2014**, *26*, 3014.
[48] Y. Z. Zhang, S. Liu, G. C. Li, G. R. Li, X. P. Gao, *J. Mater. Chem. A* **2014**, *2*, 4652.
[49] C. Zhu, H. Zhang, C. Shi, S. Li, *Constr. Build. Mater.* **2017**, *146*, 30.
[50] W. Jiang, X. Gong, S. Wang, Q. Chen, H. Zhou, W. Jiang, S. Xuan, *Appl. Phys. Lett.* **2014**, *104*, 121915.
[51] X. Liang, G. Chen, I. M. Lei, P. Zhang, Z. Wang, X. Chen, M. Lu, J. Zhang, Z. Wang, T. Sun, Y. Lan, J. Liu, *Adv. Mater.* **2022**, *35*, 2207587.
[52] K. Liu, L. Cheng, N. Zhang, H. Pan, X. Fan, G. Li, Z. Zhang, D. Zhao, J. Zhao, X. Yang, Y. Wang, R. Bai, Y. Liu, Z. Liu, S. Wang, X. Gong, Z. Bao, G. Gu, W. Yu, X. Yan, *J. Am. Chem. Soc.* **2021**, *143*, 1162.
[53] J. P. Gong, *Science* **2014**, *344*, 161.
[54] W. Wang, S. Wang, J. Zhou, H. Deng, S. Sun, T. Xue, Y. Ma, X. Gong, *Adv. Funct. Mater.* **2023**, *33*, 2202193.
[55] C. Xu, Y. Wang, J. Wu, S. Song, S. Cao, S. Xuan, W. Jiang, X. Gong, *Compos. Sci. Technol.* **2017**, *153*, 168.
[56] C. Zhao, X. Gong, S. Wang, W. Jiang, S. Xuan, *Cell Rep. Phys. Sci.* **2020**, *1*, 100266.
[57] H. Xiang, X. Li, B. Wu, S. Sun, P. Wu, *Adv. Mater.* **2023**, *35*, 2209581.
[58] J. M. Klosowski, A. T. Wolf, *The history of sealants*, CRC Press, Boca Raton, Florida, **2009**.
[59] J. M. Klosowski, *Sealants in construction*, CRC Press, Boca Raton, Florida, **2014**.
[60] https://www.marketsandmarkets.com/Market-Reports/waterproof-adhensive-and-sealants-market-3205867 (accessed: July 2022).
[61] M. A. Rahman, C. Bowland, S. Ge, S. R. Acharya, S. Kim, V. R. Cooper, X. C. Chen, S. Irle, A. P. Sokolov, A. Savara, T. Saito, *Sci Adv* **2021**, *7*, eabk2451.
[62] H. J. Meredith, C. L. Jenkins, J. J. Wilker, *Adv. Funct. Mater.* **2014**, *24*, 3259.